

Vector and axialvector mesons at nonzero temperature within a gauged linear sigma model

Stefan Strüber*

*Institut für Theoretische Physik, Johann Wolfgang Goethe-Universität,
Max von Laue-Str. 1, D-60438 Frankfurt/Main, Germany*

Dirk H. Rischke†

*Institut für Theoretische Physik and Frankfurt Institute for Advanced Studies,
Johann Wolfgang Goethe-Universität, Max von Laue-Str. 1, D-60438 Frankfurt/Main, Germany*

(Dated: February 1, 2008)

We consider vector and axialvector mesons in the framework of a gauged linear sigma model with chiral $U(N_f)_R \times U(N_f)_L$ symmetry. For $N_f = 2$, we investigate the behavior of the chiral condensate and the meson masses as a function of temperature by solving a system of coupled Dyson-Schwinger equations derived via the 2PI formalism in double-bubble approximation. We find that the inclusion of vector and axialvector mesons tends to sharpen the chiral transition. Within our approximation scheme, the mass of the ρ meson increases by about 100 MeV towards the chiral transition.

I. INTRODUCTION

The fundamental theory of the strong interaction is quantum chromodynamics (QCD). QCD has a local $SU(3)_c$ gauge symmetry which determines the interaction between matter constituents, the quarks, and gauge fields, the gluons. For massless quarks, the quark sector of the QCD Lagrangian also has a global $U(N_f)_R \times U(N_f)_L$ chiral symmetry, where N_f is the number of quark flavors. The $U(1)_A$ anomaly induced by instantons [1] breaks this symmetry explicitly to $U(N_f)_V \times SU(N_f)_A \times Z(N_f)_A$, where vector and axial vector symmetries are introduced via $V = R + L$, $A = R - L$. The discrete $Z(N_f)_A$ symmetry plays no role for the dynamics and will be omitted in the following. Nonzero, degenerate quark masses explicitly break $SU(N_f)_A$, such that the remaining symmetry is $U(N_f)_V$. Non-degenerate quark masses further break this symmetry to $U(1)_V$, corresponding to baryon number conservation.

At low momenta $\sim \Lambda_{\text{QCD}}$, where $\Lambda_{\text{QCD}} \sim 200$ MeV is the QCD scale parameter, quarks and gluons are confined inside hadrons. Therefore, on a typical hadronic length scale $\sim \Lambda_{\text{QCD}}^{-1} \sim 1$ fm, the $SU(3)_c$ gauge symmetry of QCD is (at best) of minor importance, and the interactions between hadrons are predominantly determined by the global $U(N_f)_R \times U(N_f)_L$ chiral symmetry of QCD. In the QCD vacuum, the axial $U(N_f)_A$ part of the latter symmetry is spontaneously broken by a non-vanishing expectation value of the quark condensate $\langle \bar{q}q \rangle \neq 0$ [2]. According to Goldstone's theorem, this would lead to N_f^2 Goldstone bosons. However, since the explicit symmetry breaking induced by the $U(1)_A$ anomaly reduces the axial symmetry to $SU(N_f)_A$, spontaneous symmetry breaking of the latter gives rise to only $N_f^2 - 1$ Goldstone bosons. These Goldstone bosons acquire a mass due to the explicit chiral symmetry breaking by nonzero quark masses.

At temperatures of the order of $\sim \langle \bar{q}q \rangle^{1/3}$, the thermal excitation energy is large enough to restore the $SU(N_f)_A$ symmetry of QCD. If instantons are sufficiently screened [3], this could additionally lead to a restoration of the explicitly broken $U(1)_A$. For vanishing quark masses, the high- and the low-temperature phases of QCD have different symmetries, and therefore must be separated by a phase transition. The order of this chiral phase transition is determined by the global symmetry

*Electronic address: strueber@th.physik.uni-frankfurt.de

†Electronic address: drischke@th.physik.uni-frankfurt.de

of the QCD Lagrangian; for $U(N_f)_R \times U(N_f)_L$, the transition is of first order if $N_f \geq 2$, for $SU(N_f)_R \times SU(N_f)_L \times U(1)_V$, the transition can be of second order if $N_f \leq 2$ [4]. If the quark masses are nonzero, the second-order phase transition becomes cross-over.

Lattice QCD calculations predict the chiral phase transition to happen at a temperature $T_c \sim 150 - 190$ MeV [5, 6] for zero quark chemical potential μ . The phase transition temperature is expected to decrease when μ increases and vanishes at some value μ_c corresponding to quark number densities of the order of a few times nuclear matter density. Therefore, the chiral transition of QCD is the only phase transition in a theory of one of the fundamental forces of nature which can be studied under laboratory conditions: heavy-ion collision experiments performed at the accelerator facilities CERN-SPS, BNL-RHIC and, in the near future, CERN-LHC and GSI-FAIR create matter which is sufficiently hot and/or dense, such that chiral symmetry is restored. Indeed, the primary goal of these experiments is to find evidence for the restoration of chiral symmetry by the creation of the so-called quark-gluon plasma, i.e., the phase of QCD where quarks and gluons are liberated from confinement.

When chiral symmetry is restored, the masses of hadrons with the same quantum numbers except for parity and G-parity, so-called chiral partners, become degenerate. Chiral partners are, for instance, the sigma and the pion in the (pseudo-)scalar sector, or the ρ and the a_1 in the (axial) vector sector. A promising signal for chiral symmetry restoration in heavy-ion collisions is therefore to study changes of the spectral properties of hadrons in the hot and dense environment [7–9]. One of the prime candidates is the ρ meson. The ρ meson decays sufficiently fast (and with – for experimental purposes – sufficiently large branching ratio) into a pair of dileptons which, due to their small (since electromagnetic) cross section, are able to carry information from the hot and dense stages of a heavy-ion collision to the detector. The CERES and NA60 experiments at the CERN-SPS have found convincing evidence for a modification of the ρ meson spectral function in Pb+Pb and In+In collisions, respectively [10, 11].

It is important to clarify whether the modification of the ρ meson spectral function observed by the CERN-SPS experiments is in any way related to chiral symmetry restoration or is merely due to many-body interactions in the hot and dense medium. This question can be decided by calculating the dilepton production rate from QCD and then using this rate in a dynamical model for heavy-ion collisions in order to compute the dilepton spectrum. The low-invariant mass region of the dilepton spectrum is dominated by the decay of hadronic states. Therefore, for the calculation of the dilepton rate it is more convenient to apply a low-energy effective theory for QCD, featuring hadronic states as elementary degrees of freedom and respecting the chiral symmetries of QCD, rather than using QCD itself. Since we are interested in the restoration of chiral symmetry at nonzero temperature, the low-energy effective theory of choice is a linear sigma model which treats hadrons and their chiral partners on the same footing.

Linear sigma models have been used for quite some time in order to study chiral symmetry restoration in hot and dense strongly interacting matter. For instance, Pisarski and Wilczek have applied renormalization group arguments to a $U(N_f)_V \times U(N_f)_A$ symmetric linear sigma model with scalar degrees of freedom and have drawn important qualitative conclusions regarding the order of the chiral phase transition for different numbers of quark flavors [4]. The calculation of hadronic properties at nonzero temperature (and density) faces serious technical difficulties. For instance, for the following reasons it is impossible to apply standard perturbation theory. First, it turns out that the coupling constants of effective low-energy models of QCD are of the order of one, rendering a perturbative series in the coupling constant unreliable. Second, nonzero temperature (or density) introduces an additional scale which invalidates the usual power counting in terms of the coupling constant [12]. A consistent calculation to a given order in the coupling constant then may require a resummation of whole classes of diagrams [13].

A convenient technique to perform such a resummation and thus arrive at a particular many-body approximation scheme is the so-called two-particle irreducible (2PI) or Cornwall-Jackiw-Tomboulis (CJT) formalism [14], which is a relativistic generalisation of the Φ functional formalism [15, 16]. The 2PI formalism extends the concept of the generating functional $\Gamma[\phi]$ for one-particle irreducible (1PI) Green's functions to that of one for 2PI Green's functions $\Gamma[\phi, G]$, where ϕ and G are the

expectation values of the one- and two-point functions. The central quantity in this formalism is the sum of all 2PI vacuum diagrams, $\Gamma_2[\phi, G]$. Any many-body approximation scheme can be derived as a particular truncation of $\Gamma_2[\phi, G]$.

An advantage of the 2PI formalism is that it avoids double counting and fulfills detailed balance relations and thus is thermodynamically consistent. Another advantage is that the Noether currents are conserved for an arbitrary truncation of Γ_2 as long as the one- and two-point functions transform as rank-1 and -2 tensors. A disadvantage is that Ward-Takahashi identities for higher-order vertex functions are no longer fulfilled [17]. As a consequence, Goldstone's theorem is violated [18, 19]. Another consequence is that sum rules of the Weinberg type at zero and nonzero temperature [20] are not necessarily fulfilled. A strategy to restore Goldstone's theorem is to perform a so-called "external" resummation of random-phase-approximation diagrams with internal lines given by the full propagators of the underlying approximation in the 2PI formalism [17]. In this work, however, this problem is less severe since we shall only focus on the case of explicit chiral symmetry breaking by (small) non-vanishing quark masses.

Effective theories with chiral $U(N_f)_R \times U(N_f)_L$ and $O(N)$ symmetry have already been studied within the 2PI formalism in the so-called double-bubble approximation which gives rise to Hartree-Fock-type self-energies for the individual particles [18, 19, 21–26]. The $O(N)$ model has also been studied within the 2PI formalism beyond the double-bubble approximation including sunset-type diagrams [27]. The chiral models in these works, however, only include scalar and pseudoscalar particles. Here, we extend these investigations to vector and axial vector mesons.

Our ultimate goal is a calculation of the dilepton rate for given temperature (and density). In this work, we perform the first step in this direction studying chiral symmetry restoration in the mesonic mass spectrum at nonzero temperature. We apply the so-called gauged linear sigma model as outlined in Ref. [28]. This model has been used by Pisarski [7] who varied the tree-level mass parameters in order to derive qualitative statements about the behavior of meson masses as a function of temperature. Here, we extend these studies to a full-fledged self-consistent many-body calculation of meson masses at nonzero temperature using the 2PI formalism in double-bubble approximation.

This paper is organized as follows. The following section is dedicated to a discussion of the gauged linear sigma model with $U(N_f)_R \times U(N_f)_L$ chiral symmetry, with N_f being the number of quark flavors. In Sec. III we consider the case $N_f = 2$ in more detail and rewrite the Lagrangian explicitly in terms of scalar, pseudoscalar, vector, and axial vector degrees of freedom. We also discuss issues related to the breaking of chiral symmetry such as the mixing of pseudoscalar and axial vector mesons. In Sec. IV we use this model to calculate the behavior of the meson masses and the condensate as a function of temperature. Section V concludes this paper with a summary of our results and an outlook for further studies.

We use the imaginary-time formalism to compute quantities at nonzero temperature. Our notation is

$$\int_k f(k) = T \sum_{n=-\infty}^{\infty} \int \frac{d^3k}{(2\pi)^3} f(2\pi inT, \vec{k}) . \quad (1)$$

We use units $\hbar = c = k_B = 1$. The metric tensor is $g^{\mu\nu} = \text{diag}(1, -1, -1, -1)$.

II. THE GAUGED LINEAR SIGMA MODEL

In this section we present the gauged linear sigma model with $U(N_f)_R \times U(N_f)_L$ symmetry. The Lagrangian reads [28]

$$\begin{aligned} \mathcal{L} = & \text{Tr}[(D^\mu \Phi)^\dagger D_\mu \Phi] - m_0^2 \text{Tr}[\Phi^\dagger \Phi] - \lambda_1 (\text{Tr}[\Phi^\dagger \Phi])^2 - \lambda_2 \text{Tr}[(\Phi^\dagger \Phi)^2] - \frac{1}{4} \text{Tr}[(L^{\mu\nu})^2 + (R^{\mu\nu})^2] \\ & + \frac{m_1^2}{2} \text{Tr}[(L^\mu)^2 + (R^\mu)^2] + c [\det(\Phi) + \det(\Phi^\dagger)] + \text{Tr}[H(\Phi + \Phi^\dagger)] . \end{aligned} \quad (2)$$

Here, the field Φ stands for scalar and pseudoscalar hadronic degrees. These are chosen to be organized into representations $[N_f^*, N_f]$ under $U(N_f)_R \times U(N_f)_L$ transformations, such that

$$\Phi \rightarrow U_R^\dagger \Phi U_L, \quad (3)$$

where $U_{R,L}$ are unitary matrices acting on the fundamental representation of $U(N_f)_{R,L}$. This allows for an explicit representation of Φ in terms of a complex $N_f \times N_f$ matrix,

$$\Phi = (\sigma_a + i\pi_a) T_a, \quad (4)$$

where T_a , $a = 0, \dots, N_f^2 - 1$, are the generators of $U(N_f)$ in the fundamental representation, and σ_a, π_a , parametrize scalar and pseudoscalar fields, respectively.

In order to introduce vector and axialvector degrees of freedom, one defines right- and left-handed vector fields,

$$R^\mu = (V_a^\mu + A_a^\mu) T_a, \quad L^\mu = (V_a^\mu - A_a^\mu) T_a, \quad (5)$$

where V_a^μ, A_a^μ are vector and axialvector fields, respectively. These are treated as massive Yang-Mills fields, with field-strength tensor

$$R^{\mu\nu} = \partial^\mu R^\nu - \partial^\nu R^\mu - ig [R^\mu, R^\nu], \quad L^{\mu\nu} = \partial^\mu L^\nu - \partial^\nu L^\mu - ig [L^\mu, L^\nu]. \quad (6)$$

Right- and left-handed fields transform as gauge fields under $U(N_f)_{R,L}$,

$$R^\mu \rightarrow U_R^\dagger \left(R^\mu + \frac{i}{g} \partial^\mu \right) U_R, \quad L^\mu \rightarrow U_L^\dagger \left(L^\mu + \frac{i}{g} \partial^\mu \right) U_L, \quad (7)$$

while the field-strength tensors transform covariantly under $U(N_f)_{R,L}$,

$$R^{\mu\nu} \rightarrow U_R^\dagger R^{\mu\nu} U_R, \quad L^{\mu\nu} \rightarrow U_L^\dagger L^{\mu\nu} U_L. \quad (8)$$

The covariant derivative in Eq. (2) couples scalar and pseudoscalar degrees of freedom to right- and left-handed vector fields,

$$D_\mu \Phi = \partial_\mu \Phi + ig(\Phi L_\mu - R_\mu \Phi). \quad (9)$$

The first line in Eq. (2) contains terms which are invariant under *local* $U(N_f)_R \times U(N_f)_L$ transformations. The vector meson mass term renders this symmetry a global one. The determinant terms represent the $U(1)_A$ anomaly of QCD and break the symmetry explicitly to $SU(N_f)_R \times SU(N_f)_L \times U(1)_V$, where $U(1)_V$ stands for baryon number conservation. The last term in Eq. (2) corresponds to the quark mass term in the QCD Lagrangian. Since this term is flavor-diagonal, we have $H = \sum_{i=1}^{N_f} h_{i^2-1} T_{i^2-1}$. For degenerate nonzero quark masses, $h_0 \neq 0$, while all other h_{i^2-1} vanish. In this case, $U(N_f)_R \times U(N_f)_L$ is explicitly broken to $U(N_f)_V$. For non-degenerate quark masses, also the other h_{i^2-1} have to be nonzero. Exact $SU(2)_V$ isospin symmetry requires $h_3 = 0$.

Local $U(N_f)_R \times U(N_f)_L$ invariance implies universality of the coupling, i.e., the coupling g between right- and left-handed vector fields to scalar and pseudoscalar fields is the same as the coupling of the vector fields among themselves. Note that the Lagrangian (2) would also be locally invariant under $U(N_f)_R \times U(N_f)_L$, had we introduced *separate* coupling constants g_R, g_L for right- and left-handed vector fields and modified the covariant derivative, $D_\mu \Phi = \partial_\mu \Phi + i(g_L \Phi L_\mu - g_R R_\mu \Phi)$. However, if $g_R \neq g_L$, one obtains non-vanishing parity-violating terms $\sim g_R - g_L$ in the Lagrangian, which must not occur in viable theories of the strong interaction.

The assumption of local invariance further restricts possible couplings between scalar and vector mesons. Under global transformations, terms like ΦL^μ and $R^\mu \Phi$ would transform as Φ itself. Taking discrete symmetries into account possible coupling terms would be $\text{Tr} |\Phi L^\mu - R^\mu \Phi|^2$, $\text{Tr} |\Phi L^\mu + R^\mu \Phi|^2$ and $\text{Tr} (|\Phi L^\mu|^2 + |R^\mu \Phi|^2)$ [7].

According to Noether's theorem, continuous symmetries lead to conserved currents. Explicit symmetry breaking induces source terms in the conservation laws. For global symmetries, there is a simple way to derive the currents and the conservation laws [29]. Consider the symmetry transformation to be of the form $U = \exp(-i\theta_a T_a)$. Promoting the global symmetry to a local one, $\theta_a \rightarrow \theta_a(X)$, and computing the variation $\delta\mathcal{L}$ of the Lagrangian, one can then read off the Noether currents \mathcal{J}_a^μ and the conservation laws from the identity

$$\delta\mathcal{L} = -\partial_\mu \mathcal{J}_a^\mu \theta_a - \mathcal{J}_a^\mu \partial_\mu \theta_a . \quad (10)$$

For QCD, the $U(N_f)_R \times U(N_f)_L = U(N_f)_V \times U(N_f)_A$ symmetry leads to the following vector and axial-vector currents and the conservation laws:

$$\mathcal{J}_{V\mu}^a = -\frac{\partial\delta\mathcal{L}_{QCD}}{\partial(\partial_\mu\theta_V^a)} = \bar{q}\gamma^\mu T_a q , \quad (11a)$$

$$\mathcal{J}_{A\mu}^a = -\frac{\partial\delta\mathcal{L}_{QCD}}{\partial(\partial_\mu\theta_A^a)} = \bar{q}\gamma^\mu\gamma_5 T_a q , \quad (11b)$$

$$\partial_\mu \mathcal{J}_{V\mu}^{a\mu} = -\frac{\partial\delta\mathcal{L}_{QCD}}{\partial\theta_V^a} = i\bar{q} [M, T_a] q , \quad (11c)$$

$$\partial_\mu \mathcal{J}_{A\mu}^{a\mu} = -\frac{\partial\delta\mathcal{L}_{QCD}}{\partial\theta_A^a} = i\bar{q} \{T_a, M\} \gamma_5 q + \delta_{a0} \frac{g^2 N_f}{64\pi^2} \epsilon_{\mu\nu\alpha\beta} G_b^{\mu\nu} G_b^{\alpha\beta} , \quad (11d)$$

where M is the quark mass matrix and $G_b^{\mu\nu}$ the gluon field-strength tensor. The last term on the right-hand side of the conservation law for the axial current cannot be obtained from the variation of the classical QCD Lagrangian. It represents the $U(1)_A$ anomaly and arises from instantons [1].

In the gauged linear sigma model, the vector and axial-vector currents and the corresponding conservation laws can be obtained analogously from the variation of the Lagrangian (2) under local $U(N_f)_V \times U(N_f)_A$ transformations. The result is

$$\mathcal{J}_{V\mu}^a = -\frac{\partial\delta\mathcal{L}}{\partial(\partial_\mu\theta_V^a)} = \frac{m_1^2}{g} V_\mu^a , \quad \mathcal{J}_{A\mu}^a = -\frac{\partial\delta\mathcal{L}}{\partial(\partial_\mu\theta_A^a)} = \frac{m_1^2}{g} A_\mu^a , \quad (12a)$$

$$\partial_\mu \mathcal{J}_{V\mu}^{a\mu} = -\frac{\partial\delta\mathcal{L}}{\partial\theta_V^a} = -f_{abc}\sigma_b h_c , \quad \partial_\mu \mathcal{J}_{A\mu}^{a\mu} = -\frac{\partial\delta\mathcal{L}}{\partial\theta_A^a} = d_{abc}\pi_b h_c + 4\delta_{a0} c \text{Im} [\det(\Phi)] , \quad (12b)$$

where f_{abc}, d_{abc} are the totally antisymmetric and symmetric structure constants of $SU(N)$, respectively. Since the first line in Eq. (2) is *locally* invariant under $U(N_f)_V \times U(N_f)_A$, it cannot contribute to the currents or the conservation laws. Then, the vector meson mass term which violates local $U(N_f)_V \times U(N_f)_A$ invariance gives rise to the celebrated current-field proportionality (12a) [28].

One may wonder why the vector current, $\tilde{\mathcal{J}}_{V\mu}^a$, and axial vector current, $\tilde{\mathcal{J}}_{A\mu}^a$, arising from scalar and pseudoscalar particles do not appear in the expressions (12a) for the vector and axial vector currents. They read explicitly

$$\tilde{\mathcal{J}}_{V\mu}^a = -\frac{1}{2} f_{abc} [\phi_b^* (D_\mu\phi)_c - (D_\mu\phi)_b^* \phi_c] , \quad (13a)$$

$$\tilde{\mathcal{J}}_{A\mu}^a = -\frac{i}{2} d_{abc} [\phi_b^* (D_\mu\phi)_c - (D_\mu\phi)_b^* \phi_c] , \quad (13b)$$

where

$$(D_\mu\phi)_a \equiv [\partial_\mu\delta_{ac} + g(f_{abc}V_\mu^b - id_{abc}A_\mu^b)] \phi_c \quad (14)$$

is the covariant derivative. However, employing the equations of motion, these currents are recognized as simply being parts of the total vector and axial vector currents (12a),

$$\mathcal{J}_{V\mu}^a = \tilde{\mathcal{J}}_{V\mu}^a - \frac{1}{g} \partial^\nu V_{\nu\mu}^a - f_{abc} (V_b^\nu V_{\nu\mu}^c + A_b^\nu A_{\nu\mu}^c) , \quad (15a)$$

$$\mathcal{J}_{A\mu}^a = \tilde{\mathcal{J}}_{A\mu}^a - \frac{1}{g} \partial^\nu A_{\nu\mu}^a - f_{abc} (V_b^\nu A_{\nu\mu}^c + A_b^\nu V_{\nu\mu}^c) , \quad (15b)$$

where

$$V_{\mu\nu}^a \equiv \partial_\mu V_\nu^a - \partial_\nu V_\mu^a + g f_{abc} (V_\mu^b V_\nu^c + A_\mu^b A_\nu^c) , \quad (16a)$$

$$A_{\mu\nu}^a \equiv \partial_\mu A_\nu^a - \partial_\nu A_\mu^a + g f_{abc} (V_\mu^b A_\nu^c + A_\mu^b V_\nu^c) \quad (16b)$$

are the field strength tensors for vector and axial vector fields, respectively.

In the following, we briefly discuss consequences of Eqs. (12b). In the chiral limit, $h_a = 0$, and the isosinglet vector current $\mathcal{J}_{V\mu}^0$ and the vector currents $\mathcal{J}_{V\mu}^i$, $i \neq 0$, as well as the axial vector currents $\mathcal{J}_{A\mu}^i$, are exactly conserved. The isosinglet axial vector current $\mathcal{J}_{A\mu}^0$ receives a contribution from the $U(1)_A$ anomaly. In the case of explicit chiral symmetry breaking, we have $h_a \neq 0$. However, since $f_{0bc} = 0$, the isosinglet vector current is still exactly conserved. If only $h_0 \neq 0$, but $h_i = 0$, $i \neq 0$, for the same reason also the other vector currents \mathcal{J}_V^i are exactly conserved. For instance, this is the case for $N_F = 2$ assuming isospin invariance which requires $h_i = 0$ for $i = 1, 2, 3$. In contrast, since $d_{ab0} = \delta_{ab}$, the axial vector currents are only partially conserved; the famous partial conservation of axial currents (PCAC).

III. THE CASE $N_F = 2$

So far, the discussion of the Lagrangian (2) was valid for an arbitrary number of quark flavours. In the following, we restrict ourselves to the case of mass-degenerate up and down quarks. For this case, the fields Φ , R^μ , and L^μ can be written in terms of the physical scalar (σ , \vec{a}_0), pseudoscalar (η , $\vec{\pi}$), as well as vector (ω^μ , $\vec{\rho}^\mu$) and axial vector fields (f_1^μ , $\vec{a}_{1\mu}$) as:

$$\Phi = (\sigma_a + i\pi_a) t_a = (\sigma + i\eta) t_0 + (\vec{a}_0 + i\vec{\pi}) \cdot \vec{t} , \quad (17a)$$

$$R^\mu = (V_a^\mu + A_a^\mu) t_a = (\omega^\mu + f_1^\mu) t_0 + (\vec{\rho}^\mu + \vec{a}_{1\mu}) \cdot \vec{t} , \quad (17b)$$

$$L^\mu = (V_a^\mu - A_a^\mu) t_a = (\omega^\mu - f_1^\mu) t_0 + (\vec{\rho}^\mu - \vec{a}_{1\mu}) \cdot \vec{t} . \quad (17c)$$

The vector and axial vector mesons enter the Lagrangian through the following terms:

$$\begin{aligned} \text{Tr}[(D^\mu \Phi)^\dagger D_\mu \Phi] &= \frac{1}{2} [\partial_\mu \sigma + g(\eta f_{1\mu} + \vec{\pi} \cdot \vec{a}_{1\mu})]^2 \\ &+ \frac{1}{2} [\partial_\mu \eta - g(\sigma f_{1\mu} + \vec{a}_0 \cdot \vec{a}_{1\mu})]^2 \\ &+ \frac{1}{2} [\partial_\mu \vec{a}_0 + g(\vec{\rho}_\mu \times \vec{a}_0 + \eta \vec{a}_{1\mu} + \vec{\pi} f_{1\mu})]^2 \\ &+ \frac{1}{2} [\partial_\mu \vec{\pi} - g(\vec{\pi} \times \vec{\rho}_\mu + \sigma \vec{a}_{1\mu} + \vec{a}_0 f_{1\mu})]^2 , \end{aligned} \quad (18a)$$

$$\begin{aligned} -\frac{1}{4} \text{Tr}[(L^{\mu\nu})^2 + (R^{\mu\nu})^2] &= -\frac{1}{4} (\partial_\mu \omega_\nu - \partial_\nu \omega_\mu)^2 \\ &- \frac{1}{4} (\partial_\mu f_{1\nu} - \partial_\nu f_{1\mu})^2 \\ &- \frac{1}{4} [\partial_\mu \vec{\rho}_\nu - \partial_\nu \vec{\rho}_\mu + g(\vec{\rho}_\mu \times \vec{\rho}_\nu + \vec{a}_{1\mu} \times \vec{a}_{1\nu})]^2 \\ &- \frac{1}{4} [\partial_\mu \vec{a}_{1\nu} - \partial_\nu \vec{a}_{1\mu} + g(\vec{\rho}_\mu \times \vec{a}_{1\nu} + \vec{a}_{1\mu} \times \vec{\rho}_\nu)]^2 , \end{aligned} \quad (18b)$$

$$\frac{m_1^2}{2} \text{Tr}[(L^\mu)^2 + (R^\mu)^2] = \frac{m_1^2}{2} (\omega_\mu^2 + \vec{\rho}_\mu^2 + f_{1\mu}^2 + \vec{a}_{1\mu}^2) . \quad (18c)$$

Note that the ω -meson completely decouples from the dynamics. In order to have non-vanishing coupling of the ω to the other fields, we would have to include the Wess-Zumino-Witten term [30, 31]. Note that, had we included globally $U(N_f)_V \times U(N_f)_A$ -invariant terms such as e.g. $\text{Tr} |\Phi L^\mu + R^\mu \Phi|^2$, the ω -meson would not decouple.

Since the ω -meson is protected by the $U(1)_V$ symmetry, it does not mix with the f_1 . Consequently, we do not expect the ω to become degenerate in mass with the f_1 when chiral symmetry is restored. This is in contrast to the ρ and the a_1 , which mix under $SU(2)_R \times SU(2)_L$ transformations: these mesons are expected to become degenerate in mass when chiral symmetry is restored.

In the phase where chiral symmetry is broken, the σ -field assumes a non-vanishing expectation value, $\langle \sigma \rangle \equiv \phi = \text{const.} \neq 0$. In order to examine the fluctuations around the ground state, we shift the σ -field by its vacuum expectation value, $\sigma \rightarrow \sigma + \phi$. After this shift the covariant terms (18a) read

$$\begin{aligned} \text{Tr}[(D^\mu \Phi)^\dagger D_\mu \Phi] &= \frac{1}{2} [\partial_\mu \sigma + g(\eta f_{1\mu} + \vec{\pi} \cdot \vec{a}_{1\mu})]^2 \\ &+ \frac{1}{2} [\partial_\mu \eta - g(\sigma f_{1\mu} + \phi f_{1\mu} + \vec{a}_0 \cdot \vec{a}_{1\mu})]^2 \\ &+ \frac{1}{2} [\partial_\mu \vec{a}_0 + g(\vec{\rho}_\mu \times \vec{a}_0 + \eta \vec{a}_{1\mu} + \vec{\pi} f_{1\mu})]^2 \\ &+ \frac{1}{2} [\partial_\mu \vec{\pi} - g(\vec{\pi} \times \vec{\rho}_\mu + \sigma \vec{a}_{1\mu} + \phi \vec{a}_{1\mu} + \vec{a}_0 f_{1\mu})]^2. \end{aligned} \quad (19)$$

The shift of the σ -field leads (after an integration by parts) to the bilinear terms $g\phi\eta\partial_\mu f_1^\mu$ and $g\phi\vec{\pi} \cdot \partial_\mu \vec{a}_1^\mu$. Physically, these terms correspond to a mixing between the longitudinal component of the axial vector mesons and the Goldstone modes arising from chiral symmetry breaking. If the mesons were true gauge fields, i.e., $m_1 = 0$, and if $c = H = 0$, the theory would be invariant under $U(N_f)_R \times U(N_f)_A$ gauge transformations. In this case, the mixing could be removed by an 't Hooft gauge-fixing term

$$\mathcal{L}_{GF} = -\frac{1}{2\xi}(\partial_\mu \omega^\mu)^2 - \frac{1}{2\xi}(\partial_\mu \vec{\rho}^\mu)^2 - \frac{1}{2\xi}(\partial_\mu f_1^\mu + \xi g \phi \eta)^2 - \frac{1}{2\xi}(\partial_\mu \vec{a}_1^\mu + \xi g \phi \vec{\pi})^2. \quad (20)$$

In unitary gauge, $\xi \rightarrow \infty$, the pseudoscalar particles (the Goldstone modes from spontaneously breaking $U(N_f)_V \times U(N_f)_A$ to $U(N_f)_V$) would become infinitely heavy, i.e, they are no longer dynamical degrees of freedom.

Since $m_1 \neq 0$, the 't Hooft gauge-fixing procedure is not at our disposal. We follow a method commonly used in the literature [7, 28, 32], which is a redefinition of the axial fields,

$$f_1^\mu = f_1'^\mu + w \partial^\mu \eta, \quad (21a)$$

$$\vec{a}_1^\mu = \vec{a}_1'^\mu + w \partial^\mu \vec{\pi}, \quad (21b)$$

where the new fields are denoted by a prime (which is later omitted) and w is defined such that the bilinear terms mixing the axial vector and pseudoscalar fields are eliminated,

$$w = \frac{g\phi}{m_1^2 + (g\phi)^2}. \quad (22)$$

One could also perform a redefinition of the axial vector fields using covariant derivatives [28, 32],

$$f_1^\mu = f_1'^\mu + w (\partial^\mu \eta - g \vec{a}_1'^\mu \cdot \vec{a}_0), \quad (23a)$$

$$\vec{a}_1^\mu = \vec{a}_1'^\mu + w [\partial^\mu \vec{\pi} - g (\vec{\pi} \times \vec{\rho}^\mu + g f_1'^\mu \vec{a}_0)]. \quad (23b)$$

Note, however, that the old fields appear in the covariant derivatives and couple the set of equations. Solving for the old fields in terms of the new one obtains

$$f_1^\mu = (f_1'^\mu + w \{ \partial^\mu \eta - g \vec{a}_0 \cdot [\vec{a}_1'^\mu + w (\partial^\mu \vec{\pi} + g \vec{\rho}^\mu \times \vec{\pi})] \}) (1 - g^2 w^2 \vec{a}_0^2)^{-1}, \quad (24a)$$

$$\vec{a}_1^\mu = (\vec{a}_1'^\mu + w \{ \partial^\mu \vec{\pi} - g [\vec{\pi} \times \vec{\rho}^\mu + \vec{a}_0 (f_1'^\mu + w \partial^\mu \eta)] \}) \cdot (1 - g^2 w^2 \vec{a}_0 \vec{a}_0)^{-1}. \quad (24b)$$

Note that the term $\vec{a}_0 \vec{a}_0$ on the right-hand side in Eq. (24b) is a dyadic product, and consequently the corresponding term in parentheses a matrix in isospin space, which has to be multiplied from the left

with the preceding isospin vector. The ensuing set of equations couples different isospin components of the old and new a_1 fields. All this can be avoided by simply performing the redefinition with the partial derivative, Eq. (21). It should be noted that such complications did not arise in previous treatments [28, 32], because they did not consider the η , \vec{a}_0 , and f_1 mesons. In that case, the redefinition of the a_1 field simply reads $\vec{a}_1^\mu = \vec{a}_1^{\prime\mu} + w (\partial^\mu \vec{\pi} + g \vec{\rho}^\mu \times \vec{\pi})$. It has been noted in Ref. [32] that this gives the correct seagull term when coupling the vector mesons to the photon. However, in this work we are not concerned with coupling the vector mesons to leptonic currents, and thus we restrict the consideration to the simpler version (21) of the redefinition. A different method to cope with the problem is to define a non-diagonal propagator [33].

After the redefinition (21), the kinetic terms of the pseudoscalar mesons acquire a wave-function renormalization,

$$\frac{1}{2} (\partial_\mu \pi_a)^2 \longrightarrow \frac{1}{2} Z^{-2} (\partial_\mu \pi_a)^2, \quad (25)$$

where

$$Z^2 = \frac{m_1^2 + (g\phi)^2}{m_1^2}. \quad (26)$$

In order to have correctly normalized asymptotic states, we have to redefine the pseudoscalar fields,

$$\pi_a \longrightarrow Z \pi_a. \quad (27)$$

After the redefinition of the pseudoscalar particles the Lagrangian reads

$$\begin{aligned} \mathcal{L} = & \frac{1}{2} [\partial_\mu \sigma + gZ (\eta f_{1\mu} + wZ\eta \partial_\mu \eta + \vec{\pi} \cdot \vec{a}_{1\mu} + wZ\vec{\pi} \cdot \partial_\mu \vec{\pi})]^2 \\ & + \frac{1}{2} [(\partial_\mu \eta)^2 + g^2 (\sigma f_{1\mu} + wZ\sigma \partial_\mu \eta + \vec{a}_0 \cdot \vec{a}_{1\mu} + wZ\vec{a}_0 \cdot \partial_\mu \vec{\pi})^2 \\ & \quad - 2g (Z\partial^\mu \eta - g\phi f_1^\mu - g\phi wZ\partial^\mu \eta) (\sigma f_{1\mu} + wZ\sigma \partial_\mu \eta + \vec{a}_0 \cdot \vec{a}_{1\mu} + wZ\vec{a}_0 \cdot \partial_\mu \vec{\pi})] \\ & + \frac{1}{2} [\partial_\mu \vec{a}_0 + g (\vec{\rho}_\mu \times \vec{a}_0 + Z\eta \vec{a}_{1\mu} + wZ^2\eta \partial_\mu \vec{\pi} + Z\vec{\pi} f_{1\mu} + wZ^2\vec{\pi} \partial_\mu \eta)]^2 \\ & + \frac{1}{2} [(\partial_\mu \vec{\pi})^2 + g^2 (Z\vec{\pi} \times \vec{\rho}_\mu + \sigma \vec{a}_{1\mu} + wZ\sigma \partial_\mu \vec{\pi} + \vec{a}_0 f_{1\mu} + wZ\vec{a}_0 \partial_\mu \eta)^2 \\ & \quad - 2g (Z\partial^\mu \vec{\pi} - g\phi \vec{a}_1^\mu - g\phi wZ\partial^\mu \vec{\pi}) \cdot (Z\vec{\pi} \times \vec{\rho}_\mu + \sigma \vec{a}_{1\mu} + wZ\sigma \partial_\mu \vec{\pi} + \vec{a}_0 f_{1\mu} + wZ\vec{a}_0 \partial_\mu \eta)] \\ & - \frac{1}{4} (\partial_\mu \omega_\nu - \partial_\nu \omega_\mu)^2 - \frac{1}{4} (\partial_\mu f_{1\nu} - \partial_\nu f_{1\mu})^2 \\ & - \frac{1}{4} \{ \partial_\mu \vec{\rho}_\nu - \partial_\nu \vec{\rho}_\mu + g [\vec{\rho}_\mu \times \vec{\rho}_\nu + \vec{a}_{1\mu} \times \vec{a}_{1\nu} + wZ (\vec{a}_{1\mu} \times \partial_\nu \vec{\pi} + \partial_\mu \vec{\pi} \times \vec{a}_{1\nu}) + w^2 Z^2 \partial_\mu \vec{\pi} \times \partial_\nu \vec{\pi}] \}^2 \\ & - \frac{1}{4} \{ \partial_\mu \vec{a}_{1\nu} - \partial_\nu \vec{a}_{1\mu} + g [\vec{\rho}_\mu \times \vec{a}_{1\nu} + \vec{a}_{1\mu} \times \vec{\rho}_\nu + wZ (\vec{\rho}_\mu \times \partial_\nu \vec{\pi} + \partial_\mu \vec{\pi} \times \vec{\rho}_\nu)] \}^2 \\ & - \frac{1}{2} \left[m_0^2 - c + 3 \left(\lambda_1 + \frac{\lambda_2}{2} \right) \phi^2 \right] \sigma^2 - \frac{Z^2}{2} \left[m_0^2 + c + \left(\lambda_1 + \frac{\lambda_2}{2} \right) \phi^2 \right] \eta^2 \\ & - \frac{1}{2} \left[m_0^2 + c + \left(\lambda_1 + 3 \frac{\lambda_2}{2} \right) \phi^2 \right] \vec{a}_0^2 - \frac{Z^2}{2} \left[m_0^2 - c + \left(\lambda_1 + \frac{\lambda_2}{2} \right) \phi^2 \right] \vec{\pi}^2 \\ & + \frac{m_1^2}{2} (\omega_\mu^2 + \vec{\rho}_\mu^2) + \frac{m_1^2 + (g\phi)^2}{2} (f_{1\mu}^2 + \vec{a}_{1\mu}^2) \\ & - \frac{1}{4} \left(\lambda_1 + \frac{\lambda_2}{2} \right) (\sigma^2 + Z^2 \eta^2 + \vec{a}_0^2 + Z^2 \vec{\pi}^2)^2 - \left(\lambda_1 + \frac{\lambda_2}{2} \right) \phi \sigma (\sigma^2 + Z^2 \eta^2 + \vec{a}_0^2 + Z^2 \vec{\pi}^2) \\ & - \frac{\lambda_2}{2} [(\sigma \vec{a}_0 + Z^2 \eta \vec{\pi})^2 + Z^2 \vec{a}_0^2 \vec{\pi}^2 - Z^2 (\vec{a}_0 \cdot \vec{\pi})^2] - \lambda_2 \phi \vec{a}_0 \cdot (\sigma \vec{a}_0 + Z^2 \eta \vec{\pi}) \\ & - V(\phi), \end{aligned} \quad (28)$$

where

$$V(\phi) = \frac{1}{2}(m_0^2 - c)\phi^2 + \frac{1}{4}\left(\lambda_1 + \frac{\lambda_2}{2}\right)\phi^4 - h_0\phi \quad (29)$$

is the classical potential energy density. In the derivation of Eq. (28), we have exploited the fact that ϕ is the minimum of the potential energy density, i.e.,

$$0 = \frac{dV}{d\phi} = \left[m_0^2 - c + \left(\lambda_1 + \frac{\lambda_2}{2}\right)\phi^2\right]\phi - h_0. \quad (30)$$

From the Lagrangian (28), one reads off the tree-level masses for the scalar, pseudoscalar, vector, and axial vector mesons,

$$m_\sigma^2 = m_0^2 - c + 3\left(\lambda_1 + \frac{\lambda_2}{2}\right)\phi^2, \quad (31a)$$

$$m_\eta^2 = Z^2\left[m_0^2 + c + \left(\lambda_1 + \frac{\lambda_2}{2}\right)\phi^2\right], \quad (31b)$$

$$m_{a_0}^2 = m_0^2 + c + \left(\lambda_1 + 3\frac{\lambda_2}{2}\right)\phi^2, \quad (31c)$$

$$m_\pi^2 = Z^2\left[m_0^2 - c + \left(\lambda_1 + \frac{\lambda_2}{2}\right)\phi^2\right], \quad (31d)$$

$$m_\omega^2 = m_\rho^2 = m_1^2, \quad (31e)$$

$$m_{f_1}^2 = m_{a_1}^2 = m_1^2 + (g\phi)^2. \quad (31f)$$

Note the factor Z^2 in the definition of the (squared) mass for the pseudoscalar particles. We conclude that the wave-function renormalization factor Z in Eq. (26) is equal to the ratio of the tree-level masses of the a_1 and the ρ meson, $Z \equiv m_{a_1}/m_\rho$. In the framework of this model, the difference in mass of the two mesons is due to the Higgs effect.

Using the expression for the pion mass, we obtain from Eq. (30) that $h_0 = Z^{-2}m_\pi^2\phi$. Using the renormalization of the pion field (27), the second Eq. (12b) reads $\partial_\mu \mathcal{J}_A^{i\mu} = Z^{-1}m_\pi^2\phi\pi_i$. From the PCAC relation $\partial_\mu \mathcal{J}_A^{i\mu} = f_\pi m_\pi^2\pi_i$ we then conclude that the vacuum expectation value of the scalar field is

$$\phi = Z f_\pi \equiv f_\pi \frac{m_{a_1}}{m_\rho}. \quad (32)$$

Note that the KSFR relation [34]

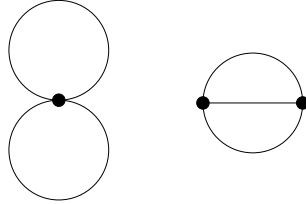
$$\frac{g^2 f_\pi^2}{m_\rho^2} = \frac{1}{2} \quad (33)$$

makes a definite prediction for Z , and thus for the relation between the mass of the ρ and the a_1 : Eqs. (26), (32), and (33) imply that $Z = \sqrt{2}$, or that $m_{a_1} = \sqrt{2}m_\rho$. For $m_\rho \simeq 770$ MeV, this means that $m_{a_1} \simeq 1090$ MeV, somewhat smaller than the value quoted by the PDG [35], $m_{a_1} \simeq 1230$ MeV.

The vector and axial vector mesons are massive spin-one particles, i.e., they have three physical degrees of freedom. In order to have an invertible inverse tree-level propagator for these particles, we have to promote the unphysical fourth degree of freedom of the vector and axial vector fields to a physical degree of freedom by adding a Stueckelberg term,

$$\mathcal{L}_{St} = -\frac{\xi}{2}\left[(\partial_\mu\omega^\mu)^2 + (\partial_\mu f_1^\mu)^2 + (\partial_\mu\bar{\rho}^\mu)^2 + (\partial_\mu\bar{a}_1^\mu)^2\right]. \quad (34)$$

The unphysical degrees of freedom can be removed by taking the limit $\xi \rightarrow 0$ at the end of the calculation.

FIG. 1: Two-loop order diagrams in V_2 .

IV. THERMAL MESON MASSES

In this section we investigate chiral symmetry restoration at nonzero temperature in the framework of the model (28). We explicitly compute the condensate and the meson masses as functions of temperature. As mentioned in the introduction, we use the 2PI resummation scheme, or Φ -functional [16], or CJT formalism [14]. The generating functional for 2PI Green's functions is

$$\Gamma[\phi, G] = S[\phi] + \frac{1}{2}\text{Tr} \ln G^{-1} + \frac{1}{2}\text{Tr} (D^{-1}G - 1) + \Gamma_2[\phi, G] , \quad (35)$$

where ϕ and G are the expectation values of the one- and two-point functions in the presence of external sources, $S[\phi]$ is the tree-level action, D^{-1} is the tree-level propagator and $\Gamma_2[\phi, G]$ is the sum of all 2PI vacuum diagrams with internal lines given by G . If the system is translationally invariant, it suffices to consider the effective potential $V = -T\Gamma/\Omega$, where T is the temperature and Ω the 3-volume of the system.

For the Lagrangian (28) the effective potential is given by

$$V[\phi, G_i] = V(\phi) + I_\sigma + I_\eta + 3I_{a_0} + 3I_\pi + I_\omega + I_{f_1} + 3I_\rho + 3I_{a_1} + V_2[\phi, G_i] , \quad (36)$$

where $V_2 = -T\Gamma_2/\Omega$, and

$$I_i = \frac{1}{2} \int_k [\ln G_i^{-1}(k) + \mathcal{D}_i^{-1}(k)G_i(k) - 1] , \quad (37)$$

with the inverse tree-level propagators for scalar particles $\mathcal{D}_i^{-1} = -k^2 + m_i^2$, $i = \sigma, \eta, a_0, \pi$, and for vector particles $\mathcal{D}_{i\ \mu\nu}^{-1} = -(k^2 - m_i^2)g_{\mu\nu} + (1 - \xi)k_\mu k_\nu$, $i = \omega, f_1, \rho, a_1$. The condensate ϕ and the full propagators G_i are determined from the stationarity conditions for the effective potential (36),

$$\frac{\delta V}{\delta \phi} = 0 , \quad \frac{\delta V}{\delta G_i} = 0 . \quad (38)$$

The last equation is identical to the Dyson-Schwinger equation for the full propagators,

$$G_i^{-1} = D_i^{-1} + \Pi_i , \quad (39)$$

where the 1PI self-energy Π_i is given by

$$\Pi_i = -2 \frac{\delta V_2}{\delta G_i} . \quad (40)$$

To lowest order in the loop expansion, i.e., to two-loop order, two types of diagrams contribute to V_2 . The diagram in Fig. 1, made of a single four-point vertex, is called the double-bubble diagram. The other one, made of two three-point vertices, is called the sunset diagram. In Eq. (40), the functional derivative of V_2 with respect to a full propagator is diagrammatically equivalent to cutting a line

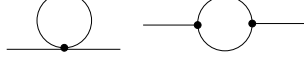


FIG. 2: 1PI self-energy II.

corresponding to that propagator. This gives rise to the self-energy diagrams shown in Fig. 2. In contrast to the sunset diagram, the double-bubble diagram does not produce an imaginary part in the 1PI self-energy when analytically continuing the latter to real energies. Thus, it gives only constant (temperature-dependent) corrections to the mass and the wave-function renormalization constant of the particle. Neglecting the sunset terms is, of course, still a self-consistent approximation in the framework of the 2PI formalism. The advantage is that it tremendously reduces the numerical effort: instead of solving a set of coupled complex integral equations for the self-energy functions $\Pi(k_0, \vec{k})$ for a given temperature, one only has to solve a set of coupled real fixed-point equations for the masses and wave-function renormalization constants.

For the Lagrangian (28), we explicitly list V_2 in double-bubble approximation in Eq. (A1) of App. A. As detailed in that appendix, we make a further approximation to simplify the structure of the vertices corresponding to interactions of vector and axial vector mesons with themselves and with pions. This approximation yields degenerate dispersion relations for transverse and longitudinal (axial-) vector degrees of freedom. The resulting self-energies are given in Eqs. (A6), and the set of coupled fixed-point equations in Eqs. (A7).

The parameters of the model are fixed to the vacuum masses and the pion decay constant. Without vacuum fluctuations, vacuum and tree-level masses are identical, and we have

$$\lambda_1 = \frac{1}{2(Zf_\pi)^2} \left[m_\sigma^2 - \left(\frac{m_\pi}{Z} \right)^2 - m_{a_0}^2 + \left(\frac{m_\eta}{Z} \right)^2 \right], \quad (41a)$$

$$\lambda_2 = \frac{1}{(Zf_\pi)^2} \left[m_{a_0}^2 - \left(\frac{m_\eta}{Z} \right)^2 \right], \quad (41b)$$

$$m_0^2 = \left(\frac{m_\pi}{Z} \right)^2 + \frac{1}{2} \left[\left(\frac{m_\eta}{Z} \right)^2 - m_\sigma^2 \right], \quad (41c)$$

$$c = \frac{m_\eta^2 - m_\pi^2}{2Z^2}, \quad (41d)$$

$$h_0 = \frac{f_\pi m_\pi^2}{Z}, \quad (41e)$$

$$m_1^2 = m_\rho^2, \quad (41f)$$

$$g^2 = \frac{m_{a_1}^2 - m_\rho^2}{(Zf_\pi)^2}, \quad (41g)$$

with

$$\begin{aligned} m_\sigma &= 400 - 1400 \text{ MeV}, \\ m_\eta &= 547.75 \text{ MeV}, \\ m_{a_0} &= 985.1 \text{ MeV}, \\ m_\pi &= 138.04 \text{ MeV}, \\ m_\rho &= 768.5 \text{ MeV}, \\ m_{a_1} &= m_{f_1} = 1230 \text{ MeV}, \\ f_\pi &= 91.9 \text{ MeV}. \end{aligned}$$

In Figs. 3 and 4 we show the temperature dependence of the condensate and the scalar meson masses without the influence of vector mesons, i.e., setting $g = 0$ (and $Z = 1$). In Fig. 3, we choose a vacuum

sigma mass of $m_\sigma = 441$ MeV [36]. This leads to a cross-over phase transition at $T_c \simeq 193$ MeV, in good agreement with the lattice QCD calculations of Ref. [6].

Taking a vacuum sigma mass of $m_\sigma = 1370$ MeV (which is another candidate for a 0^{++} state [35]), the phase transition is of first order at a critical temperature of $T_c \simeq 238$ MeV, cf. Fig. 4. Within this scenario with only scalar, but no vector mesons, we obtain a second-order phase transition for a critical sigma mass of about $m_\sigma^* \simeq 965$ MeV at a temperature of $T_c \simeq 222$ MeV.

In Figs. 5 and 6, we show the meson masses, the condensate, and the wave-function renormalization constants as functions of temperature including vector meson degrees of freedom. For $m_\sigma = 441$ MeV, cf. Fig. 5, we observe a cross-over transition at about the same temperature, $T_c \simeq 195$ MeV, as in the pure scalar case. However, the inclusion of vector mesons leads to a more rapid cross-over. This is a typical effect within chiral linear σ models when including more dynamical degrees of freedom, e.g., strange and charmed scalar mesons [22]. Including vector mesons this effect is even stronger.

The increasing steepness of the cross-over transition indicates that the inclusion of vector mesons brings one closer to a second-order critical point. This can also be seen comparing the value of the σ mass at the respective transition temperature in Figs. 3 and 5. In the latter, the σ meson is lighter by about 100 MeV. At a second-order critical point, the σ should become completely massless [37], indicating a diverging correlation length. Moving closer to a second-order critical point by the inclusion of vector degrees of freedom is advantageous from the following point of view. Let us consider the second-order critical endpoint of the line of first-order phase transitions associated with the restoration of chiral symmetry, or shortly, the QCD critical point. Usually, in chiral models of QCD, this point is located at temperatures which are too small and quark chemical potentials which are too large [38] as compared to lattice QCD calculations [39]. Our calculations are performed at $\mu = 0$. The fact that the inclusion of vector mesons brings one closer to a second-order phase transition indicates that the QCD critical point moves closer to the T axis in the $T - \mu$ plane. We thus conjecture that the inclusion of vector mesons in linear σ models improves the agreement with lattice QCD.

Note that the ρ mass increases, and the a_1 mass decreases, as a function of temperature, until these mesons become degenerate in mass beyond the chiral symmetry restoring transition. This is a necessary requirement for chiral symmetry restoration, as argued in Ref. [7]. The question remains, whether the mass of the ρ increases to meet that of the a_1 , or whether both decrease (or, for that matter, increase) with T , before becoming degenerate. In our model, the increase of M_ρ with T is not surprising, because it consists of two separate contributions, the tree-level mass parameter m_1 , and the contributions from thermal (tadpole) fluctuations. While the former is constant as a function of temperature, one can show that the latter are always non-negative, therefore the mass of the ρ has no choice but to increase with temperature. This would be different, though, had we chosen to generate the tree-level mass dynamically through chiral symmetry breaking [32]. In this case, the tree-level contribution would decrease as the condensate melts, while the thermal tadpole contributions would increase. (To our knowledge, this argument was first given in Ref. [8].) As the condensate goes to zero in the process of chiral symmetry restoration, only the latter survive and lead to an increase of M_ρ with T . Nevertheless, in this scenario, at intermediate temperatures one cannot exclude that the ρ meson mass first decreases with T , assumes a minimum, and then increases again. The minimum value of M_ρ may well be zero, as advertised by models with hidden gauge symmetry [40].

The pion and η wave-function renormalization constants are unity at $T = 0$, and then increase by about 10 % (for the pion) or 20 % (for the η) when approaching the chiral phase transition. They sharply drop back to one when the transition temperature is exceeded.

In Fig. 6 we show the thermal masses, the condensate, and the wave-function renormalization for $m_\sigma = 1370$ MeV. In this case, there is a first-order phase transition at $T_c \simeq 258$ MeV. For the sake of completeness we note that the second-order phase transition now occurs for a critical sigma mass $m_\sigma^* \simeq 795$ MeV at a temperature of $T_c \simeq 220$ MeV, i.e., at smaller values of m_σ and T_c than without vector mesons.

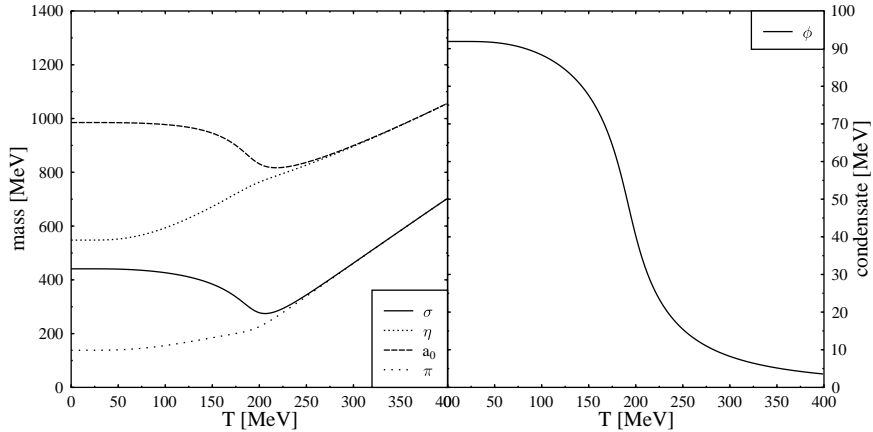


FIG. 3: Masses for scalar and pseudoscalar mesons (left panel) and chiral condensate (right panel) as a function of temperature for the case $g = 0$, $m_\sigma = 441$ MeV.

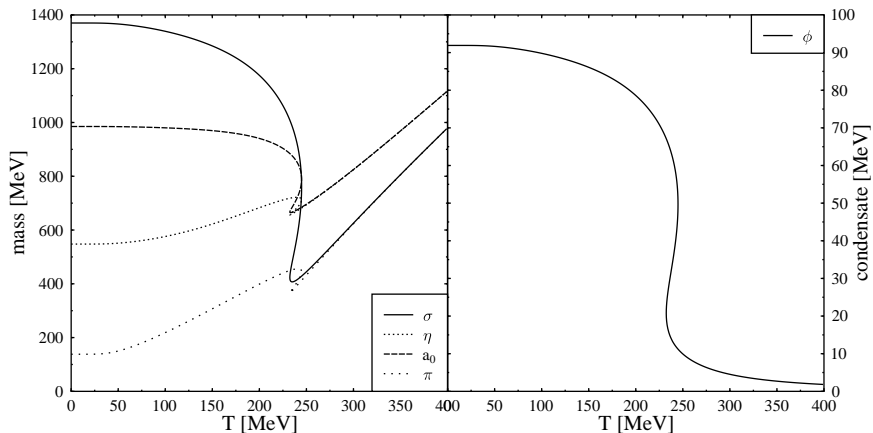


FIG. 4: The same as in Fig. 3, for $m_\sigma = 1370$ MeV.

V. CONCLUSIONS

In this work, we have investigated an effective theory for QCD with chiral $U(2)_R \times U(2)_L$ symmetry. Besides scalar and pseudoscalar degrees of freedom, we included vector and axial vector mesons. These were coupled minimally to the scalar and pseudoscalar mesons. The ensuing local $U(2)_R \times U(2)_L$ symmetry is explicitly broken to the corresponding global symmetry by introducing a mass term for vector and axial vector mesons. Without introducing a Wess-Zumino-Witten term, it turns out that the ω meson completely decouples from the theory.

In the Goldstone phase, a non-vanishing chiral condensate leads to terms bilinear in the axial vector and pseudoscalar fields. Lacking the freedom to choose a convenient (i.e., 't Hooft) gauge, in order to get rid of these terms one can perform a redefinition of the axial vector fields with a subsequent redefinition of the pseudoscalar degrees of freedom.

The resulting Lagrangian was employed to derive a set of coupled Dyson-Schwinger equations

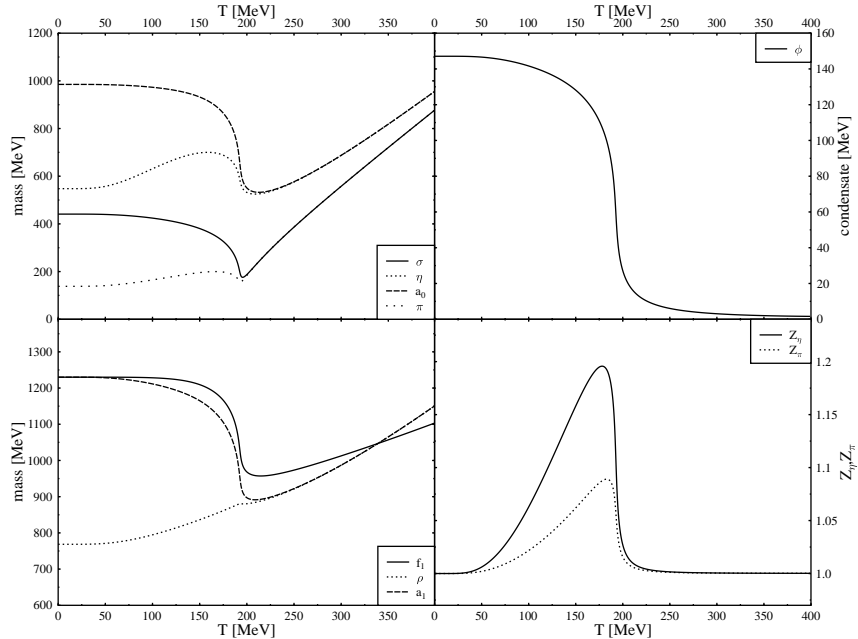


FIG. 5: Masses for scalar and pseudoscalar mesons (upper left panel), for vector and axial vector mesons (lower left panel), the chiral condensate (upper right panel), and the pion and η wave-function renormalization constants as a function of temperature for the full model including vector and axial vector degrees of freedom; $m_\sigma = 441$ MeV.

via the 2PI formalism. In this work, we approximate the 2PI effective potential by including only the so-called double-bubble diagrams. This leads to constant, temperature-dependent shifts of the masses and, in the case of the pseudoscalar mesons, the wave-function renormalization constants.

We did a control calculation without vector and axial vector meson degrees of freedom in order to study the influence of the latter on the chiral phase transition. We found that, without vector mesons, and with a vacuum sigma mass $m_\sigma = 441$ MeV, there is a smooth cross-over phase transition at a critical temperature of $T_c \simeq 193$ MeV. In the case with vector mesons, this cross-over transition becomes sharper, however, the transition temperature remains approximately the same, $T_c \simeq 195$ MeV.

Increasing the mass of the sigma, the phase transition becomes sharper and turns into a first-order transition beyond a critical sigma mass m_σ^* . At m_σ^* , the transition is second of order. For the case without vector mesons, this happens for $m_\sigma^* \simeq 965$ MeV, with a critical temperature of $T_c \simeq 222$ MeV. For the case with vector mesons, this happens already for a smaller critical sigma mass, $m_\sigma^* \simeq 795$ MeV with a critical temperature of $T_c \simeq 220$ MeV. The fact that m_σ^* becomes smaller when including vector mesons can be understood from the fact that, for a given m_σ , the transition was found to become sharper as compared to the case without vector mesons. This indicates that the inclusion of vector mesons brings one closer to a second-order critical point.

This has consequences for the location of the QCD critical point in the $T - \mu$ phase diagram. Without vector mesons, chiral models of QCD usually predict this point at temperatures which are too small and at quark chemical potentials which are too large as compared to lattice QCD calculations. Since our above mentioned results are obtained at $\mu = 0$, the inclusion of vector mesons would move this point closer to the T axis and thus would improve the agreement with the lattice results.

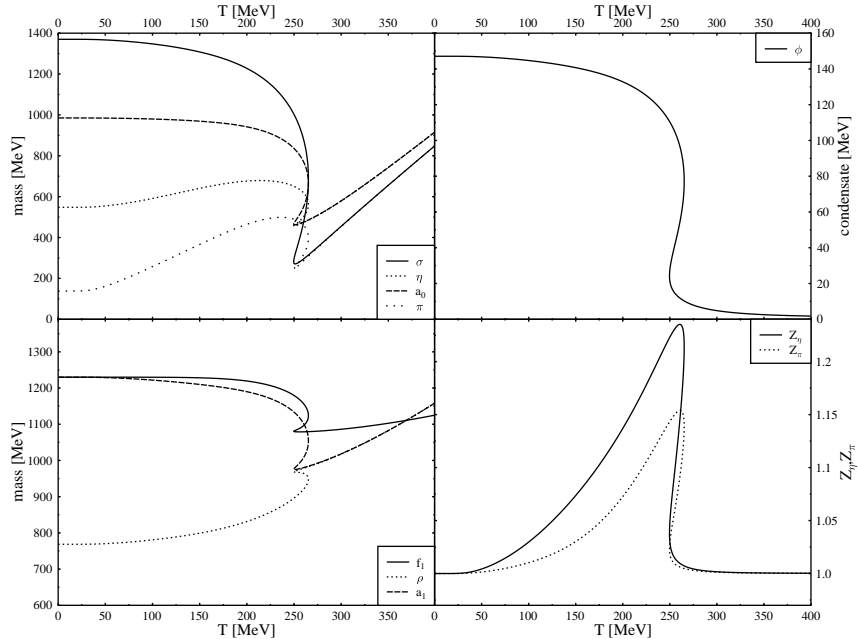


FIG. 6: Same as in Fig. 5; $m_\sigma = 1370$ MeV.

In our calculations, the mass of the ρ meson is a monotonously increasing function of temperature. This is not surprising; in our model, the mass of the ρ essentially consists of two contributions, the tree-level mass plus thermal fluctuations from tadpole diagrams. The former is always constant, while the latter are positive definite and, in general, increasing functions of temperature. A qualitatively different scenario would be one where the tree-level mass is also generated dynamically through spontaneous symmetry breaking. A self-consistent treatment of this case within the Hartree approximation could be a topic of future studies. However, the generic feature of chiral symmetry restoration, namely that the ρ and the a_1 become degenerate in mass at the chiral phase transition, should still hold for this case.

The ultimate goal is to find signatures for chiral symmetry restoration in hot and dense nuclear matter as created in heavy-ion collisions. In this context, a promising observable is the invariant mass spectrum of dileptons, since they carry direct information from the hot and dense stages of the evolution of the system. Of particular interest is the contribution of the ρ meson to the dilepton spectrum, since it has a large (vacuum) decay width and therefore decays inside the medium. Changes of the spectral properties of the ρ meson potentially related to chiral symmetry restoration can thus be directly seen in the dilepton invariant mass spectrum.

With this in mind, the present study should be extended along several lines. In the double-bubble approximation to the 2PI effective action, the quasiparticle self-energy has no imaginary part. Thus, in this approximation the quasiparticles cannot decay. A natural next step is therefore to include sunset-type diagrams in the 2PI effective action, which lead to nonzero imaginary parts for the self-energy of the quasiparticles and, in turn, to a nonzero decay width. Another possible project is the self-consistent calculation of meson masses for the gauged linear sigma model extended to the three-flavor case [28]. From previous studies of dilepton production we know that baryons play an important role [9]. Therefore, it is mandatory to include nucleons into the present model. Of course, a linear representation of chiral symmetry requires to also add the chiral partner of the nucleon as an explicit degree of freedom [41, 42]. Since the chiral partner of the nucleon is most likely heavier than

the Δ resonance, the latter is more abundant in a hot and dense system. It is therefore unavoidable to also include spin 3/2-resonances and their chiral partners [43].

Acknowledgment

The authors thank Hendrik van Hees, Robert Pisarski, Dirk Röder, Jörg Ruppert, Jürgen Schaffner-Bielich, Igor Shovkovy, and Detlev Zschiesche for valuable discussions. S.S. thanks GSI Darmstadt for support through an F&E grant.

APPENDIX A: EFFECTIVE POTENTIAL AND GAP EQUATIONS

In this appendix, we simplify our notation by denoting full propagators of a given field by the field itself, for instance $G_\sigma(k) = \sigma(k)$, $G_\rho^{\mu\nu}(k) = \rho^{\mu\nu}(k)$ etc. The trace over a vector propagator is denoted by the corresponding field without Lorentz indices, for instance $\rho_\mu^\mu(k) = \rho(k)$. With this notation, the generating functional in double-bubble approximation reads:

$$\begin{aligned}
V_2 = & \frac{1}{4} \left(\lambda_1 + \frac{\lambda_2}{2} \right) \left\{ 3 \left[\int_k \sigma(k) \right]^2 + 3Z^4 \left[\int_k \eta(k) \right]^2 + 15 \left[\int_k a_0(k) \right]^2 + 15Z^4 \left[\int_k \pi(k) \right]^2 \right. \\
& \left. + 2Z^2 \int_k \sigma(k) \int_l \eta(l) + 6Z^2 \int_k \sigma(k) \int_l \pi(l) + 6Z^2 \int_k \eta(k) \int_l a_0(l) \right\} \\
& + \frac{3}{2} \left(\lambda_1 + \frac{3\lambda_2}{2} \right) \left[\int_k \sigma(k) \int_l a_0(l) + Z^4 \int_k \eta(k) \int_l \pi(l) \right] + \frac{9}{2} Z^2 \left(\lambda_1 + \frac{7\lambda_2}{6} \right) \int_k a_0(k) \int_l \pi(l) \\
& - \frac{g^2}{2} w^2 Z^2 \left(\int_k k^2 \eta(k) \left\{ \int_l \sigma(l) + Z^2 \int_l \eta(l) + 3 \left[\int_l a_0(l) + Z^2 \int_l \pi(l) \right] \right\} \right. \\
& \left. + 3 \int_k k^2 \pi(k) \left[\int_l \sigma(l) + Z^2 \int_l \eta(l) + \int_l a_0(l) + Z^2 \int_l \pi(l) \right] \right) \\
& + \frac{3}{2} g^2 w^4 Z^4 \left\{ \left[\int_k k^2 \pi(k) \right]^2 - \int_k k^\mu k^\nu \pi(k) \int_l l_\mu l_\nu \pi(l) \right\} \\
& + \frac{g^2}{2} \left\{ \int_k f_1(k) \left[\int_l \sigma(l) + Z^2 \int_l \eta(l) + 3 \int_l a_0(l) + 3Z^2 \int_l \pi(l) \right] + 6 \int_k \rho(k) \left[\int_l a_0(l) + Z^2 \int_l \pi(l) \right] \right. \\
& \left. + 3 \int_k a_1(k) \left[\int_l \sigma(l) + Z^2 \int_l \eta(l) + \int_l a_0(l) + Z^2 \int_l \pi(l) \right] \right. \\
& \left. - 6w^2 Z^2 \left[\int_k \rho^{\mu\nu}(k) + \int_k a_1^{\mu\nu}(k) \right] \int_l (l^2 g_{\mu\nu} - l_\mu l_\nu) \pi(l) \right\} \\
& + \frac{3}{2} g^2 \left\{ \left[\int_k \rho(k) \right]^2 - \int_k \rho^{\mu\nu}(k) \int_l \rho_{\mu\nu}(l) + \left[\int_k a_1(k) \right]^2 - \int_k a_1^{\mu\nu}(k) \int_l a_{1\mu\nu}(l) \right. \\
& \left. + 2 \left[\int_k \rho(k) \int_l a_1(l) - \int_k \rho^{\mu\nu}(k) \int_l a_{1\mu\nu}(l) \right] \right\} . \tag{A1}
\end{aligned}$$

At this point we decompose the terms in V_2 derived from vectorial vertices in the following manner. Let $G_V^{\mu\nu}$ denote a vector or axial-vector propagator (with trace G_V , according to our above convention). We then decompose a rank-2 tensor structure $B^{\mu\nu}$ as follows,

$$B^{\mu\nu} = \frac{1}{4} g^{\mu\nu} B + \delta B^{\mu\nu}, \quad \delta B^{\mu\nu} = B^{\mu\nu} - \frac{1}{4} g^{\mu\nu} B, \tag{A2}$$

and apply this to $G_V^{\mu\nu}$ as well as $k^\mu k^\nu$. We then neglect terms involving $\delta B^{\mu\nu}$. This results in the replacements

$$\left[\int_k G_V(k) \right]^2 - \int_k G_V^{\mu\nu}(k) \int_l G_{V\mu\nu}(l) \longrightarrow \frac{3}{4} \left[\int_k G_V(k) \right]^2, \quad (\text{A3a})$$

$$\int_k G_V(k) \int_l l^2 \pi(l) - \int_k G_V^{\mu\nu}(k) \int_l l_\mu l_\nu \pi(l) \longrightarrow \frac{3}{4} \int_k G_V(k) \int_l l^2 \pi(l), \quad (\text{A3b})$$

$$\int_k k^2 \pi(k) \int_l l^2 \pi(l) - \int_k k^\mu k^\nu \pi(k) \int_l l_\mu l_\nu \pi(l) \longrightarrow \frac{3}{4} \left[\int_k k^2 \pi(k) \right]^2. \quad (\text{A3c})$$

In this way, the vector and axial-vector meson self-energies become proportional to $g^{\mu\nu}$, i.e., transverse and longitudinal self-energies become identical.

The condensate equation with the approximated vectorial vertices reads

$$\begin{aligned} h_0 = & \phi \left[(m_0^2 - c) + \left(\lambda_1 + \frac{\lambda_2}{2} \right) \phi^2 + 3 \left[\left(\lambda_1 + \frac{\lambda_2}{2} \right) \int_k \sigma(k) + \left(\lambda_1 + 3 \frac{\lambda_2}{2} \right) \int_k a_0(k) \right] \right. \\ & + \frac{1}{2} \left\{ \left[m_0^2 + c + \left(\lambda_1 + \frac{\lambda_2}{2} \right) \phi^2 \right] u + 2Z^2 \left(\lambda_1 + \frac{\lambda_2}{2} \right) \right\} \int_k \eta(k) \\ & + \frac{3}{2} \left\{ \left[m_0^2 - c + \left(\lambda_1 + \frac{\lambda_2}{2} \right) \phi^2 \right] u + 2Z^2 \left(\lambda_1 + \frac{\lambda_2}{2} \right) \right\} \int_k \pi(k) \\ & + g^2 \left[\int_k f_1(k) + 3 \int_k a_1(k) \right] + \frac{3}{2} \int_k \pi(k) \left[v \left(\lambda_1 + \frac{3\lambda_2}{2} \right) \int_l \eta(l) + 3u \left(\lambda_1 + \frac{7\lambda_2}{6} \right) \int_l a_0(l) \right] \\ & + \frac{1}{4} \left(\lambda_1 + \frac{\lambda_2}{2} \right) \left(2u \left[\int_k \sigma(k) \int_l \eta(l) + 3 \int_k \sigma(k) \int_l \pi(l) + 3 \int_k \eta(k) \int_l a_0(l) \right] \right. \\ & \quad \left. + 3v \left\{ \left[\int_k \eta(k) \right]^2 + 5 \left[\int_k \pi(k) \right]^2 \right\} \right) \\ & + \frac{g^2}{2} \int_k \eta(k) \left\{ u_1 \left[\int_l l^2 \eta(l) + 3 \int_l l^2 \pi(l) \right] + u \left[\int_l f_1(l) + 3 \int_l a_1(l) \right] \right\} \\ & + \frac{3}{2} g^2 \int_k \pi(k) \left\{ u_1 \left[\int_l l^2 \eta(l) + \int_l l^2 \pi(l) \right] + u \left[\int_l f_1(l) + 2 \int_k \rho(l) + \int_l a_1(l) \right] \right\} \\ & + \frac{g^2}{2} r \left\{ \int_k \sigma(k) \left[\int_l l^2 \eta(l) + 3 \int_l l^2 \pi(l) \right] + 3 \int_k a_0(k) \left[\int_l l^2 \eta(l) + \int_l l^2 \pi(l) \right] \right\} \\ & \left. + \frac{9}{4} g^2 r \int_k k^2 \pi(k) \left[\int_l \rho(l) + \int_l a_1(l) \right] + \frac{9}{8} g^2 v_1 \left[\int_k k^2 \pi(k) \right]^2 \right\}, \quad (\text{A4}) \end{aligned}$$

where

$$u = \frac{1}{\phi} \frac{d(Z^2)}{d\phi} = \frac{2g^2}{m_1^2}, \quad (\text{A5a})$$

$$v = \frac{1}{\phi} \frac{d(Z^4)}{d\phi} = \frac{4g^2 (m_1^2 + g^2 \phi^2)}{m_1^4}, \quad (\text{A5b})$$

$$r = -\frac{1}{\phi} \frac{d(w^2 Z^2)}{d\phi} = -\frac{2g^2}{(m_1^2 + g^2 \phi^2)^2}, \quad (\text{A5c})$$

$$u_1 = -\frac{1}{\phi} \frac{d(w^2 Z^4)}{d\phi} = -\frac{2g^2}{m_1^4}, \quad (\text{A5d})$$

$$v_1 = \frac{1}{\phi} \frac{d(w^4 Z^4)}{d\phi} = \frac{4g^4 \phi^2}{m_1^2 (m_1^2 + g^2 \phi^2)^3}. \quad (\text{A5e})$$

The approximation (A3) has the distinct feature that the vector-meson self-energies are proportional to the metric tensor, $\Pi_i^{\mu\nu} = g^{\mu\nu} \Pi_i$, $i = f_1, \rho, a_1$. The self-energies with the approximated vectorial vertices are

$$\begin{aligned} \Pi_\sigma &= \left(\lambda_1 + \frac{\lambda_2}{2} \right) \left\{ 3 \int_k \sigma(k) + Z^2 \left[\int_k \eta(k) + 3 \int_k \pi(k) \right] \right\} + 3 \left(\lambda_1 + 3 \frac{\lambda_2}{2} \right) \int_k a_0(k) \\ &\quad - g^2 \left\{ w^2 Z^2 \left[\int_k k^2 \eta(k) + 3 \int_k k^2 \pi(k) \right] - \int_k f_1(k) - 3 \int_k a_1(k) \right\}, \end{aligned} \quad (\text{A6a})$$

$$\begin{aligned} Z^{-2} \Pi_\eta(l) &= Z^{-2} \Pi_\eta^* + Z^{-2} l^2 \Pi_\eta^{**} \\ &= \left(\lambda_1 + \frac{\lambda_2}{2} \right) \left[\int_k \sigma(k) + 3 Z^2 \int_k \eta(k) + 3 \int_k a_0(k) \right] + 3 Z^2 \left(\lambda_1 + 3 \frac{\lambda_2}{2} \right) \int_k \pi(k) \\ &\quad - g^2 \left\{ w^2 Z^2 \left[\int_k k^2 \eta(k) + 3 \int_k k^2 \pi(k) \right] - \int_k f_1(k) - 3 \int_k a_1(k) \right\} \\ &\quad - g^2 w^2 l^2 \left\{ \int_k \sigma(k) + Z^2 \int_k \eta(k) + 3 \left[\int_k a_0(k) + Z^2 \int_k \pi(k) \right] \right\}, \end{aligned} \quad (\text{A6b})$$

$$\begin{aligned} \Pi_{a_0} &= \left(\lambda_1 + \frac{\lambda_2}{2} \right) \left[Z^2 \int_k \eta(k) + 5 \int_k a_0(k) \right] + \left(\lambda_1 + 3 \frac{\lambda_2}{2} \right) \int_k \sigma(k) + 3 Z^2 \left(\lambda_1 + 7 \frac{\lambda_2}{6} \right) \int_k \pi(k) \\ &\quad - g^2 \left\{ w^2 Z^2 \left[\int_k k^2 \eta(k) + \int_k k^2 \pi(k) \right] - \int_k f_1(k) - 2 \int_k \rho(k) - \int_k a_1(k) \right\}, \end{aligned} \quad (\text{A6c})$$

$$\begin{aligned} Z^{-2} \Pi_\pi(l) &= Z^{-2} \Pi_\pi^* + Z^{-2} l^2 \Pi_\pi^{**} \\ &= \left(\lambda_1 + \frac{\lambda_2}{2} \right) \left[\int_k \sigma(k) + 5 Z^2 \int_k \pi(k) \right] + Z^2 \left(\lambda_1 + 3 \frac{\lambda_2}{2} \right) \int_k \eta(k) + 3 \left(\lambda_1 + 7 \frac{\lambda_2}{6} \right) \int_k a_0(k) \\ &\quad - g^2 \left\{ w^2 Z^2 \left[\int_k k^2 \eta(k) + \int_k k^2 \pi(k) \right] - \int_k f_1(k) - 2 \int_k \rho(k) - \int_k a_1(k) \right\} \\ &\quad - g^2 w^2 l^2 \left\{ \int_k \sigma(k) + \int_k a_0(k) + Z^2 \left[\int_k \eta(k) + \int_k \pi(k) - \frac{3}{2} w^2 \int_k k^2 \pi(k) \right] \right. \\ &\quad \left. + \frac{3}{2} \left[\int_k \rho(k) + \int_k a_1(k) \right] \right\}, \end{aligned} \quad (\text{A6d})$$

$$\Pi_{f_1} = g^2 \left\{ \int_k \sigma(k) + 3 \int_k a_0(k) + Z^2 \left[\int_k \eta(k) + 3 \int_k \pi(k) \right] \right\}, \quad (\text{A6e})$$

$$\Pi_\rho = 2g^2 \left\{ \int_k a_0(k) + Z^2 \left[\int_k \pi(k) - \frac{3w^2}{4} \int_k k^2 \pi(k) \right] + \frac{3}{4} \left[\int_k \rho(k) + \int_k a_1(k) \right] \right\}, \quad (\text{A6f})$$

$$\begin{aligned} \Pi_{a_1} &= g^2 \left\{ \int_k \sigma(k) + \int_k a_0(k) + Z^2 \left[\int_k \eta(k) + \int_k \pi(k) - \frac{3w^2}{2} \int_k k^2 \pi(k) \right] \right. \\ &\quad \left. + \frac{3}{2} \left[\int_k \rho(k) + \int_k a_1(k) \right] \right\}. \end{aligned} \quad (\text{A6g})$$

Finally, the coupled set of fixed-point equations for the masses and wave-function renormalization

constants is given by

$$M_\sigma^2 = m_\sigma^2 + \Pi_\sigma , \quad (\text{A7a})$$

$$M_\eta^2 = m_\eta^2 + \Pi_\eta^* , \quad (\text{A7b})$$

$$-Z_\eta^2 = -1 + \Pi_\eta^{**} , \quad (\text{A7c})$$

$$M_{a_0}^2 = m_{a_0}^2 + \Pi_{a_0} , \quad (\text{A7d})$$

$$M_\pi^2 = m_\pi^2 + \Pi_\pi^* , \quad (\text{A7e})$$

$$-Z_\pi^2 = -1 + \Pi_\pi^{**} , \quad (\text{A7f})$$

$$M_{f_1}^2 = m_{f_1}^2 + \Pi_{f_1} , \quad (\text{A7g})$$

$$M_\rho^2 = m_\rho^2 + \Pi_\rho , \quad (\text{A7h})$$

$$M_{a_1}^2 = m_{a_1}^2 + \Pi_{a_1} , \quad (\text{A7i})$$

which has to be solved together with Eq. (A4). A consistent ansatz for the full propagators in momentum space is

$$G_{\sigma,a_0}(k) = -\frac{1}{k^2 - M_{\sigma,a_0}^2} , \quad (\text{A8a})$$

$$G_{\eta,\pi}(k) = -\frac{1}{Z_{\eta,\pi}^2} \frac{1}{k^2 - M_{\eta,\pi}^2/Z_{\eta,\pi}^2} , \quad (\text{A8b})$$

$$G_{f_1,\rho,a_1}^{\mu\nu}(k) = -\frac{1}{k^2 - M_{f_1,\rho,a_1}^2} g^{\mu\nu} - \frac{1}{M_{f_1,\rho,a_1}^2} \left(\frac{1}{k^2 - M_{f_1,\rho,a_1}^2/\xi} - \frac{1}{k^2 - M_{f_1,\rho,a_1}^2} \right) k^\mu k^\nu . \quad (\text{A8c})$$

The tadpole integrals emerging after the Matsubara summation are

$$T_{\sigma,a_0} = \int_k -\frac{1}{k^2 - M_{\sigma,a_0}^2} = \int \frac{d^3k}{(2\pi)^3} \frac{1 + 2n_B(\omega_{\sigma,a_0})}{2\omega_{\sigma,a_0}} , \quad (\text{A9a})$$

$$T_{\eta,\pi} = \int_k -\frac{1}{Z_{\eta,\pi}^2} \frac{1}{k^2 - M_{\eta,\pi}^2/Z_{\eta,\pi}^2} = \frac{1}{Z_{\eta,\pi}^2} \int \frac{d^3k}{(2\pi)^3} \frac{1 + 2n_B(\omega_{\eta,\pi})}{2\omega_{\eta,\pi}} , \quad (\text{A9b})$$

$$T_{\eta,\pi}^* = \int_k -\frac{1}{Z_{\eta,\pi}^2} \frac{k^2}{k^2 - M_{\eta,\pi}^2/Z_{\eta,\pi}^2} = \frac{M_{\eta,\pi}^2}{Z_{\eta,\pi}^4} \int \frac{d^3k}{(2\pi)^3} \frac{1 + 2n_B(\omega_{\eta,\pi})}{2\omega_{\eta,\pi}} , \quad (\text{A9c})$$

$$\begin{aligned} T_{f_1,\rho,a_1} &= \int_k \left[-\frac{4}{k^2 - M_{f_1,\rho,a_1}^2} - \frac{1}{M_{f_1,\rho,a_1}^2} \left(\frac{1}{k^2 - M_{f_1,\rho,a_1}^2/\xi} - \frac{1}{k^2 - M_{f_1,\rho,a_1}^2} \right) k^2 \right] \\ &= 3 \int \frac{d^3k}{(2\pi)^3} \frac{1 + 2n_B(\omega_{f_1,\rho,a_1})}{2\omega_{f_1,\rho,a_1}} + \frac{1}{\xi} \int \frac{d^3k}{(2\pi)^3} \frac{1 + 2n_B(\omega_{f_1,\rho,a_1}^\xi)}{2\omega_{f_1,\rho,a_1}^\xi} , \end{aligned} \quad (\text{A9d})$$

where $\omega_i = (\vec{k}^2 + M_i^2)^{1/2}$ for $i = \sigma, a_0, f_1, \rho, a_1$, while $\omega_i = (\vec{k}^2 + M_i^2/Z_i^2)^{1/2}$ for $i = \pi, \eta$, and $\omega_i^\xi = (\vec{k}^2 + M_i^2/\xi)^{1/2}$ for $i = \rho, a_1$; $n_B(\omega) = [\exp(\omega/T) - 1]^{-1}$ is the Bose-Einstein distribution. For the actual computation, we renormalize the tadpole integrals in such a way that divergent vacuum contributions vanish. Other renormalization prescriptions (yielding nonzero vacuum contributions) are possible, but do not lead to qualitatively different results [19]. Note that, after taking the limit $\xi \rightarrow 0$, only the three physical vector meson degrees of freedom contribute to the tadpole integrals.

[1] G. 't Hooft, Phys. Rept. **142**, 357 (1986).

[2] C. Vafa and E. Witten, Nucl. Phys. B **234**, 173 (1984).

- [3] D. J. Gross, R. D. Pisarski and L. G. Yaffe, *Rev. Mod. Phys.* **53**, 43 (1981).
- [4] R. D. Pisarski and F. Wilczek, *Phys. Rev. D* **29**, 338 (1984).
- [5] Y. Aoki, Z. Fodor, S. D. Katz and K. K. Szabo, *Phys. Lett. B* **643**, 46 (2006) [arXiv:hep-lat/0609068].
- [6] F. Karsch, arXiv:hep-ph/0701210.
- [7] R. D. Pisarski, arXiv:hep-ph/9503330.
- [8] G. E. Brown and M. Rho, arXiv:nucl-th/0509002.
- [9] R. Rapp and J. Wambach, *Adv. Nucl. Phys.* **25**, 1 (2000) [arXiv:hep-ph/9909229].
- [10] G. Agakichiev *et al.* [CERES Collaboration], *Eur. Phys. J. C* **41**, 475 (2005) [arXiv:nucl-ex/0506002].
- [11] S. Damjanovic *et al.* [NA60 Collaboration], *Nucl. Phys. A* **783**, 327 (2007) [arXiv:nucl-ex/0701015].
- [12] L. Dolan and R. Jackiw, *Phys. Rev. D* **9**, 3320 (1974).
- [13] E. Braaten and R. D. Pisarski, *Nucl. Phys. B* **337**, 569 (1990).
- [14] J. M. Cornwall, R. Jackiw and E. Tomboulis, *Phys. Rev. D* **10**, 2428 (1974).
- [15] J. M. Luttinger and J. C. Ward, *Phys. Rev.* **118**, 1417 (1960).
- [16] G. Baym, *Phys. Rev.* **127**, 1391 (1962).
- [17] H. van Hees and J. Knoll, *Phys. Rev. D* **66**, 025028 (2002) [arXiv:hep-ph/0203008].
- [18] N. Petropoulos, *J. Phys. G* **25**, 2225 (1999) [arXiv:hep-ph/9807331].
- [19] J. T. Lenaghan and D. H. Rischke, *J. Phys. G* **26**, 431 (2000) [arXiv:nucl-th/9901049].
- [20] J. I. Kapusta and E. V. Shuryak, *Phys. Rev. D* **49**, 4694 (1994) [arXiv:hep-ph/9312245].
- [21] J. T. Lenaghan, D. H. Rischke and J. Schaffner-Bielich, *Phys. Rev. D* **62**, 085008 (2000) [arXiv:nucl-th/0004006].
- [22] D. Roder, J. Ruppert and D. H. Rischke, *Phys. Rev. D* **68**, 016003 (2003) [arXiv:nucl-th/0301085].
- [23] G. Baym and G. Grinstein, *Phys. Rev. D* **15** (1977) 2897.
- [24] A. Bochkarev and J. I. Kapusta, *Phys. Rev. D* **54**, 4066 (1996) [arXiv:hep-ph/9602405].
- [25] J. Polchinski, arXiv:hep-th/9611050.
- [26] G. Amelino-Camelia, *Phys. Lett. B* **407**, 268 (1997) [arXiv:hep-ph/9702403].
- [27] D. Roder, J. Ruppert and D. H. Rischke, *Nucl. Phys. A* **775**, 127 (2006) [arXiv:hep-ph/0503042].
- [28] S. Gasiorowicz and D. A. Geffen, *Rev. Mod. Phys.* **41**, 531 (1969).
- [29] M. Gell-Mann and M. Levy, *Nuovo Cim.* **16**, 705 (1960).
- [30] J. Wess and B. Zumino, *Phys. Lett. B* **37**, 95 (1971).
- [31] O. Kaymakcalan, S. Rajeev and J. Schechter, *Phys. Rev. D* **30**, 594 (1984).
- [32] P. Ko and S. Rudaz, *Phys. Rev. D* **50**, 6877 (1994).
- [33] M. Urban, M. Buballa and J. Wambach, *Nucl. Phys. A* **697**, 338 (2002) [arXiv:hep-ph/0102260].
- [34] K. Kawarabayashi and M. Suzuki, *Phys. Rev. Lett.* **16**, 255 (1966); Riazuddin and Fayyazuddin, *Phys. Rev.* **147**, 1071 (1966).
- [35] W. M. Yao *et al.* [Particle Data Group], *J. Phys. G* **33**, 1 (2006).
- [36] H. Leutwyler, arXiv:hep-ph/0608218.
- [37] M. A. Stephanov, K. Rajagopal and E. V. Shuryak, *Phys. Rev. D* **60**, 114028 (1999) [arXiv:hep-ph/9903292].
- [38] M. A. Stephanov, arXiv:hep-lat/0701002.
- [39] Z. Fodor and S. D. Katz, *JHEP* **0404**, 050 (2004) [arXiv:hep-lat/0402006].
- [40] M. Harada and C. Sasaki, *Phys. Rev. D* **73**, 036001 (2006) [arXiv:hep-ph/0511312].
- [41] C. DeTar and T. Kunihiro, *Phys. Rev. D* **39**, 2805 (1989).
- [42] S. Wilms, F. Giacosa and D. H. Rischke, arXiv:nucl-th/0702076.
- [43] D. Jido, T. Hatsuda and T. Kunihiro, *Phys. Rev. Lett.* **84**, 3252 (2000) [arXiv:hep-ph/9910375].